# Remote sensing estimation of actual evapotranspiration and crop coefficients for a multiple land use arid landscape of southern Iran with limited available data

M. Pakparvar, W. Cornelis, L. S. Pereira, D. Gabriels, H. Hosseinimarandi, M. Edraki and S. A. Kowsar

## ABSTRACT

The Gareh Bygone Plain is an arid area, south of Zagros Mountains, in Southern Iran, where a floodwater spreading project has been implemented for artificial recharge of groundwater. Knowledge/mapping of actual evapotranspiration for the mainland uses (natural pasture, irrigated crops and tree plantations) is of major importance for water management in this remote area. The Surface Energy Balance System (SEBS) model was used to estimate actual evapotranspiration (ET) using non-cloudy images for 32 dates of Landsat 5 TM from May 2009 to October 2010. Various improvements were required for ET computations, including relative to the very high wind speed observed. Reference ET was computed with observed weather data and SEBS products. Thus, crop coefficients ($K_c$) were obtained as the ratios of actual to reference ET relative to the main types of vegetation. The mid-season $K_c$ generated with SEBS were compared with those previously obtained in the region and with those published in literature. Consumed water by cultivated crops based on SEBS compared well with applied water measurements. Coherent results were obtained which allow validating the SEBS approach for conditions of limited available data.

**Key words** | GRASS GIS, Landsat, reference evapotranspiration, SEBS model, surface energy balance, wind speed adjustments

**M. Pakparvar** (corresponding author)
**W. Cornelis**
**D. Gabriels**
Department of Soil Management,
Faculty of Bioscience Engineering,
Ghent University,
653 Coupure Links, 9000 Ghent, Belgium
E-mail: *Mojtaba.Pakparvar@UGent.be*; *Pakparvar@farsagres.ir*

**M. Pakparvar**
School of Environmental Sciences,
Charles Sturt University,
Wagga Wagga, Australia

**L. S. Pereira**
CEER – Biosystems Engineering,
Institute of Agronomy, University of Lisbon,
Portugal

**M. Edraki**
Bureau of Meteorology,
Canberra, Australia

**H. Hosseinimarandi**
**S. A. Kowsar**
Fars Research Center for Agriculture and Natural Resources,
Shiraz, Iran

## NOMENCLATURE

| | |
|---|---|
| $A_{cm}$ | coefficient for the $K_c$ adjustment |
| $d_0$ | zero plane displacement height, m |
| $e_a$ | actual vapour pressure of the water vapour, hPa |
| $e_s$ | saturated vapour pressure, hPa |
| $ET_a$ | actual evapotranspiration, mm day$^{-1}$ |
| $ET_o$ | grass reference evapotranspiration, mm day$^{-1}$ |
| $f_v$ | fraction of ground covered by vegetation |
| $G$ | soil heat flux, W m$^{-2}$ |
| $H$ | vegetation height, m |
| $H$ | sensible heat flux, W m$^{-2}$ |
| $H_{dry}$ | dry limit of sensible heat |
| $H_{wet}$ | wet limit of sensible heat |
| $K_c$ | crop coefficient |
| $K_{c\ adj}$ | adjusted $K_c$ |
| $K_{c\ mid}$ | mid-season $K_c$ |
| $K_s$ | stress coefficient |
| LAI | leaf area index, m$^2$ m$^{-2}$ |
| LST | land surface temperature |
| NDVI | Normalized Deference Vegetation Index |
| $P$ | atmospheric pressure, Pa |
| $p_v$ | vegetation proportion |
| $q$ | specific humidity, kg kg$^{-1}$ |
| RH | relative humidity, % |
| $R_n$ | net radiation, W m$^{-2}$ |
| $T$ | mean daily air temperature, °C |
| $T_a$ | air temperature, °C |
| TOA | top of atmosphere reflectance |
| $T_{rad}$ | thermal band TOA product |

doi: 10.2166/hydro.2014.140

| | |
|---|---|
| $T_s$ | surface temperature, °C |
| $u_{inst}$ | wind speed at the time of satellite overpass, m $s^{-1}$ |
| $u_{max}$ | maximum daily wind speed, m $s^{-1}$ |
| $z_{om}$ | roughness height for momentum, m |
| $\alpha$ | broadband albedo |
| $\varepsilon$ | broadband emissivity |
| $\lambda$ | latent heat of vaporization, MJ $kg^{-1}$ |
| $\lambda E$ | latent heat flux of evaporation, MJ $m^{-2}$ $day^{-1}$ |
| ARG | artificial recharge of groundwater |
| ASTER | Advanced Space borne Thermal Emission and Reflection Radiometer |
| FWS | floodwater spreading |
| GBP | Gareh Bygone Plain |
| GRASS | geographic resources analysis support system (RS-GIS software) |
| MODIS | moderate resolution imaging spectro-radiometer |
| SEBS | Surface Energy Balance System |
| RMSE | root mean square error |

## INTRODUCTION

Knowledge of actual evapotranspiration ($ET_a$) is essential for assessing the water balance, particularly in arid areas when water saving practices, such as floodwater harvesting basins for groundwater recharge, need to be evaluated. $ET_a$ varies regionally and seasonally according to environmental conditions, mainly climate, land cover and land use, soil moisture and crop management. Conventional measurement techniques using point observations to estimate evapotranspiration (ET) using the components of the energy balance (Allen *et al.* 2011) produce information representative of local scales only and are difficult to be extended to large areas due to the heterogeneity of land surfaces and the dynamic nature of heat transfer processes (Su 2002). Contrarily to local scale methods, remote sensing (RS) provides large scale information and data of a hydrological, vegetation, soil and topographic nature that help overcoming limitations relative to ground observation networks (Sun *et al.* 2009). Hence, many efforts have focused on ET estimation and mapping at various scales using RS data, particularly during the last decade (Su *et al.* 2005; Gowda *et al.* 2008; Sun *et al.* 2009).

Various RS-based ET algorithms are available for estimating ET at various time and space scales and of varied complexity. Comprehensive reviews of various land surface energy balance models have been published, e.g., Courault *et al.* (2005), Overgaard *et al.* (2006), Kalma *et al.* (2008) and Gowda *et al.* (2008). Widely tested land surface energy balance models include Surface Energy Balance Algorithm for Land (SEBAL) (Bastiaanssen *et al.* 1998), Surface Energy Balance Index (SEBI) (Menenti & Choudhury 1993), Simplified-SEBI (S-SEBI) (Roerink *et al.* 2000), Surface Energy Balance System (SEBS) (Su 2002), Two-Source Model (Norman *et al.* 1995; Chehbouni *et al.* 2001) and METRIC (Allen *et al.* 2007).

The present research refers to a floodwater spreading (FWS) project area located in the Gareh Bygone Plain (GBP), south of Zagros Mountains, in southern Iran. ET from agricultural crops and tree plantations play a major role in water use in this area. Currently, there are no reliable data on ET but, because it is a major component of the water balance of the plain, its knowledge and estimation is definitely required. Due to the complex and heterogeneous vegetation cover of the project site and difficulties in assessing ET at local scale, the RS SEBS algorithm was selected to estimate $ET_a$. Hence its estimation accuracy needs to be assessed for the conditions of this study and particularly when limited data are available.

SEBS has been evaluated over agricultural, grassland and forested sites, and across several spatial scales and with Landsat, ASTER and MODIS satellite-acquired data (Su *et al.* 2005, 2008; McCabe & Wood 2006; van der Kwast *et al.* 2009). A good consistency was observed between flux retrievals from $ETM^+$ and ASTER data but MODIS data were unable to discriminate the influence of heterogeneity in land use at field scale while results were comparable at catchment scale (McCabe & Wood 2006). Estimation accuracy of various models/algorithms is reported by Gowda *et al.* (2008), which can be as high as 94% for seasonal evapotranspiration and 97% for daily evapotranspiration. The SEBS model needs simpler parameterization than SEBAL or METRIC but is less tested than these algorithms, particularly for arid landscapes having limited ground data. Thus, particular attention has to be given to uncertainties in parameterization (Gibson *et al.* 2011; Lu *et al.* 2013).

The main objectives of this RS study are to assess the performance of the SEBS model in a hot and dry region to

estimate actual ET for various land cover types and, using ground-based reference ET, to derive appropriate crop coefficients for the vegetation of the Gareh Bygone Plain, thus to map both ET and crop coefficients for this target area. It is also aimed to further extend the use of SEBS and related information to perform the soil water balance of the area, to assess results of the FWS project and to support water management in the region.

## MATERIALS AND METHODS

### Study site

The GBP is an area of 18,000 ha. The FWS project area comprises 2,445 ha. Very little freshwater resources were available before the artificial recharge of the groundwater through the FWS activities, which started there by 1983.

The GBP is located south of the Zagros mountains, in southern Iran, between 28°35′ to 28°41′N and 53°53′ to 53°57′E. The altitude of the plain ranges between 1,120 and 1,160 m.a.s.l. (Figure 1). This is a dry region, with mean annual precipitation of 219 mm, having high inter-annual variability. Rainfall mainly occurs from December to March, with few exceptional events in summer (June–July). The maximum temperature (40–46 °C) occurs in July to August and the minimum (−1 to −6 °C) occurs in January to February (Table 1). Weather data are available from the Gareh Bygone and the Fasa weather stations. The Gareh Bygone weather station is part of the national weather stations network (OFCM 2005) and is located inside the study site (28°36′N, 53°55′ and 1,162 m altitude).

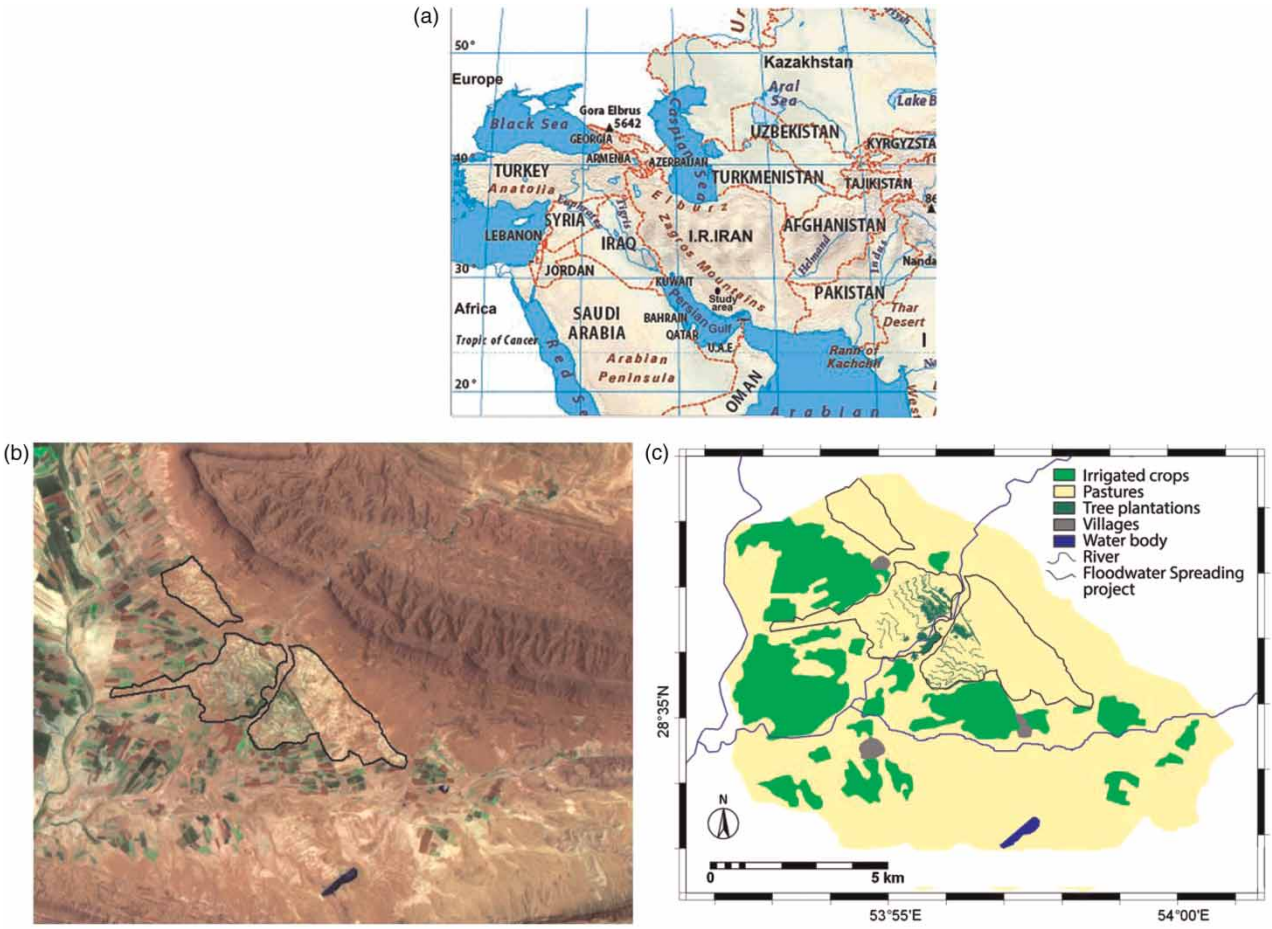


**Figure 1** | (a) Location of the study site in Iran; (b) landscape of the Gareh Bygone Plain with location of the FWS project ($RGB_{742}$ Landsat TM5 21/10/2010); (c) simplified map of main land uses. The scale bar is accurate for map (c).

**Table 1** | Representative weather data of Gareh Bygone station, 1996–2011

| Variable | Statistic | Jan | Feb | Mar | Apr | May | Jun | Jul | Aug | Sep | Oct | Nov | Dec | Year |
|---|---|---|---|---|---|---|---|---|---|---|---|---|---|---|
| Prec. (mm) | Mean | 50.2 | 44.5 | 34.1 | 28.2 | 4.0 | 1.3 | 0.6 | 6.1 | 3.6 | 0.4 | 7.7 | 38.5 | 219.2 |
| | Std | 37.7 | 47.8 | 30.4 | 29.8 | 9.0 | 3.7 | 1.7 | 9.4 | 5.6 | 1.5 | 12.8 | 47.2 | 65.5 |
| Temp (°C) | Max Abs. | 24.5 | 26.5 | 32.0 | 34.5 | 40.5 | 44.5 | 46.0 | 45.5 | 43.0 | 38.5 | 33.0 | 27.0 | 38.5 |
| | Mean | 8.0 | 9.4 | 13.1 | 17.0 | 23.3 | 28.1 | 31.9 | 31.2 | 28.0 | 22.7 | 16.3 | 10.7 | 16.6 |
| | Min Abs. | − 6.5 | − 6.0 | − 2.5 | 1.0 | 5.0 | 9.5 | 16.0 | 15.0 | 12.0 | 3.5 | − 2.0 | − 6.5 | − 6.5 |
| Frost days | Mean | 11.0 | 19.0 | 9.0 | 0.0 | 0.0 | 0.0 | 0.0 | 0.0 | 0.0 | 2.0 | 3.0 | 4.0 | 40.0 |
| RH (%) | Max | 79.0 | 80.3 | 77.0 | 71.6 | 57.3 | 48.4 | 50.3 | 49.0 | 50.8 | 53.5 | 66.5 | 77.2 | 65.7 |
| | Min | 45.0 | 38.7 | 33.1 | 32.4 | 24.3 | 18.1 | 20.5 | 20.0 | 21.7 | 24.3 | 32.4 | 43.4 | 33.4 |
| Wind ($m.s^{-1}$) | Max | 10.4 | 15.3 | 15.0 | 21.2 | 17.6 | 13.7 | 13.7 | 17.8 | 12.2 | 10.9 | 11.6 | 8.6 | 11.6 |
| | Mean | 1.6 | 2.6 | 2.4 | 3.6 | 3.3 | 3.3 | 3.3 | 2.4 | 2.6 | 2.2 | 2.0 | 1.5 | 1.9 |

The observed climatic variables are those required for computing $ET_o$ (Allen *et al.* 1998). The Fasa weather station is a synoptic station (28°58′N and 53°41′ and 1,288 altitude) located 45 km north-east of the study site, whose hourly data were available at http://www.mundomanz.com/meteo_p/main but net radiation was received through personal correspondence. Net radiation measured at the Fasa station was used to compare calculated and measured net radiation.

Irrigated crop fields in GBP have an annual crop–fallow rotation system covering nearly 2,200 ha and are mostly located in the vicinity of the FWS project. Wheat is the main winter crop, which is sometimes replaced by barley or cotton. Watermelon, melon and cantaloupe are the main mid-summer crops, which alternate with wheat or barley in rotation; forage corn is also grown in summer. By 1983 to 1987, 133 ha were planted with trees, predominantly *Eucalyptus camaldulensis* Dehnh., and scarcely the other species of eucalyptus and acacia (mainly *Acacia victoria* Benth). *E. camaldulensis* has covered more than 90% of the forested area in FWS. The remaining part of FWS is covered with pasture crops (Mesbah & Kowsar 2010). A surface reservoir covering 62 ha and created by a small earth dam was selected to extract the $ET_a$ data of open water pixels. The distribution of main land uses and overlayed field points is presented in Figure 2. Information on vegetation and general conditions during the normal years is summarized in Table 2.

The soils are classified as Torriorthents, Haplocalcids and Haplocambids Kowsar & Pakparvar (2003). More detail on soils and description of the aquifer is presented by Hashemi *et al.* (2012).

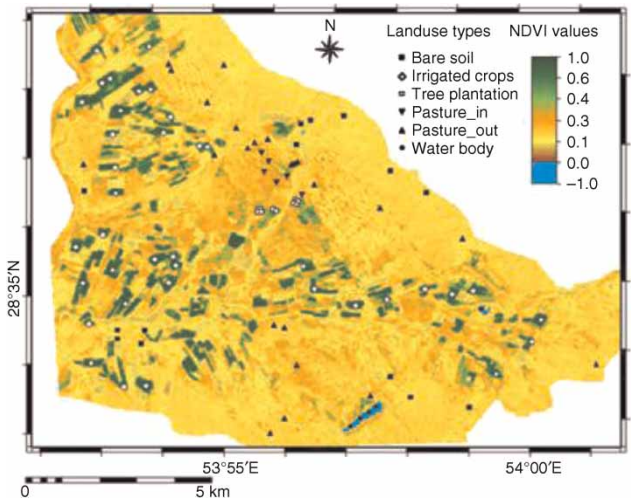


**Figure 2** | NDVI map generated from Landsat 5 on 18/03/2010 image with indication of field points of main land uses.

## Model description

The one-dimensional SEBS uses satellite and commonly available meteorological data to estimate the surface energy balance (Su 2002)

$$\lambda E = R_n - G - H \quad (1)$$

where, $\lambda E$ is latent heat flux of evaporation, $R_n$ is net radiation, $G$ is soil heat flux, and $H$ is the sensible heat flux (all in W $m^{-2}$ units) (Allen *et al.* 1998).

**Table 2** | Vegetation characteristics of the studied land use types

| | | | Agronomic dates | | | Irrigation | | |
|---|---|---|---|---|---|---|---|---|
| **Land use** | **Crop type** | **Vegetation** | **Sowing** | **Harvesting** | **Max. green canopy** | **Method** | **Depth (mm)** | **Average yield, t.ha$^{-1}$** |
| Farm lands | Winter crops | Wheat (or barley) | 20–25 Nov. | 5–10 Jun | 10–20 Apr. | Surface | 400–570 | 4–5 |
| | Mid-summer crops | Water melon, melon, cantaloupe | 20–30 Feb. | 10–15 Aug | 1–15 Aug. | Furrow | 1,100–1,300 | Different |
| | Late summer crops | Forage corn | 15–20 Aug. | 5–10 Nov. | 25 Sep. –20 Oct. | Furrow | 900–1,100 | 35–45 |
| Other land uses | | | | | | | | |
| | Plant type | Species | | Phenologic dates | | | Crown cover[1], % | |
| | | | | Start germination | Fall | Max. greenness | Inside FWS | Outside FWS |
| Pastures | Native perennials | *Helianthemum lippii Artemisia sieberi*, | | 20 Feb | 20 Oct. | 20 Apr.–5 Jun. | Max. 67; Min. 19; | Max. 30; Min. 10; |
| | Native annuals | *Aegilops cerasa, Medicago polymorpha*, *Medicago radiata* | | 10–20 Jan. | 20 May | 20 Mar.–20 Apr. | Mean 32 | Mean 19 |
| | Plantations | *Atriplex lentiformis* | | Evergreen | | 20 Mar.–30 Apr. | | |
| Tree plantations | Native | *Ziziphus nummularia* | | Evergreen | | 20 Jan.–20 May | $< 1$ | 1–3 |
| | Plantations | *Eucalyptus camaldulensis*, | | Evergreen | | 20 Jan.–20 May | 80–100 | 0 |
| | | *Acacia victoria* | | Evergreen | | 20 Jan.– 20 May | 5–10 | 0 |

[1]Based on Mesbah and Kowsar (2010).

Detailed SEBS parameterization can be found in Su *et al.* (2005). The input data requirements of SEBS refer to three sets of data, as follows.

(1) Basic RS products: albedo, emissivity, thermal band ($T_{rad}$) relative to the top of atmosphere (TOA), which can be used as LST, and Normalized Difference Vegetation Index (NDVI).
(2) Vegetation products: LAI, fraction of ground covered by vegetation ($f_v$, non-dimensional) and vegetation height ($h$). When vegetation information is not available, NDVI is used as an independent variable to generate the vegetation products.
(3) Ground observed weather data: air temperature, wind speed observed at a given height ($u$, m $s^{-1}$), actual vapour pressure ($e_a$) at a given reference height, atmospheric pressure ($P$), sunshine duration (hours), all for satellite overpass time, and mean daily temperature ($T_a$,°C) and downward solar radiation data.

Further details on the particular techniques used to separate the sensible and latent heat fluxes from the available energy are given by Su (2002).

Integrated land and water information system (ILWIS) Open 3.8.3 and the SEBS Toolbox plug-in (http://www.itc.nl/Pub/WRS/WRS-GEONETCast), which were used in this study, provide a set of routines of SEBS for biogeophysical parameter extraction. It uses satellite-based earth observation data in combination with ground-based meteorological information as inputs to produce SEBS results in the form of different maps including the actual evapotranspiration ($ET_a$).

In SEBS, in order to determine the evaporative fraction (partition of the available energy between sensible and latent), use is made of energy balance considerations at limiting cases. Under the dry-limit, the latent heat (or the evaporation) becomes zero due to the limitation of soil moisture, and the sensible heat flux ($H$) is at its maximum value using evaporative fraction. At the wet-limit, the internal resistance = 0 and the H is at a minimum. Hwet and Hdry is calculated using calculated latent heat ($\lambda E$). The model uses Menenti (1984) to find latent heat. The Penman–Monteith equation (FAO 56) is only valid for vegetation canopy, whereas Menenti's (1984) is also valid for soil surface with properly defined bulk internal resistance. Thus, the latent heat flux reflects both the soil evaporation and plant transpiration which is of great importance in arid regions.

## RS data and products

Landsat thematic mapper TM5 images were used as the source of RS for vegetation parameters and net radiation calculations. The study site is located in an area where two adjacent Landsat paths, 161 and 162, overlap; thus, potentially, it is possible to have 7 and 9 days alternate intervals of image gathering. Available images (42) from May 2009 to October 2010 for both mentioned adjacent paths of row 40 were downloaded from Glovis website (http://glovis.usgs.gov/). Mean radiance values of thermal bands for the non-cloudy images are presented in Figure 3. Excluding eight cloudy and two low quality images, 32 scenes were analysed.

All downloaded scenes for this study have been corrected at level 1 T (http://landsat.usgs.gov). The radiometric correction process including the conversion from digital numbers to radiance, was applied using the equations proposed by Chander & Markham (2003). The resulting values are reflectance at the TOA. The images were converted to earth skin reflectance through the 6S algorithm (Second Simulation of Satellite Signal in the Solar Spectrum) inside GRASS-GIS applying the 'i.atcorr' module (Neteler & Mitasova 2008). The US Standard 62 was used as atmospheric model, continental as aerosol model, and visibility number (visible distance by unarmed eye in km) recorded in Fasa weather station at the satellite over passing date and time. The aim of this process was to minimize the atmospheric effects and producing the at-surface reflectance. A script was written for Linux users to run the atmospheric correction module automatically for multiple Landsat TM5 images under analysis.

Among the RS products, albedo, emissivity and NDVI were generated by using both TOA and at-surface images to test the impact of atmospheric correction on $ET_a$ production. Thermal band TOA product $T_{rad}$ was used as land surface temperature (LST). Albedo is an integration of the surface reflectance of all of the shortwave bands assuming a coefficient for every band. Weighing coefficients proposed by Tasumi *et al.* (2008) were used in this study. Land surface emissivity (ε) was produced by the Thresholds Method $NDVI^{THM}$ proposed by Sobrino *et al.* (2004).

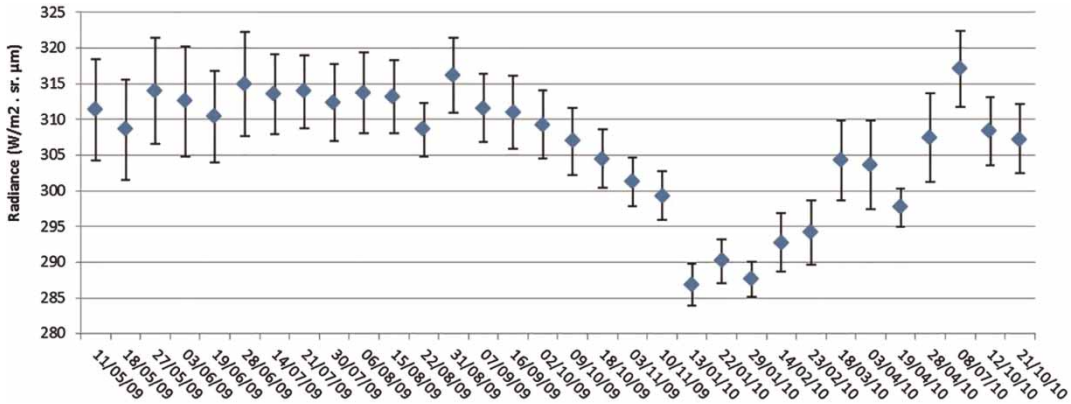


**Figure 3** | Mean values of top of atmosphere radiation for thermal band images of non-cloudy dates during the study period (scale bars are standard deviations).

This method obtains the emissivity values from the NDVI considering three different cases: (a) NDVI <0.2, in which the pixel is considered as bare soil and the emissivity is obtained from reflectivity values in the red region; (b) NDVI >0.5, in which pixels are considered as fully vegetated, and then a constant value for the emissivity is assumed, typically of 0.99; (c) 0.2 ≤NDVI ≤0.5, in which the pixel is composed of a mixture of bare soil and vegetation, and the emissivity is calculated as

$$\varepsilon = \varepsilon_v P_v + \varepsilon_s (1 - P_v) + d_\varepsilon \quad (2)$$

where, $\varepsilon$ is the emissivity, $\varepsilon_v$ is the emissivity of the vegetation, $\varepsilon_s$ is the soil emissivity, and $P_v$ is the vegetation proportion obtained according to Carlson & Ripley (1997)

$$P_v = \left[\frac{NDVI - NDVI_{min}}{NDVI_{max} - NDVI_{min}}\right]^2 \quad (3)$$

where, $NDVI_{max} = 0.8$ and $NDVI_{min} = 0.05$, which refer to observed NDVI values for fully vegetated and bare soil pixels, respectively. The term $d_\varepsilon$ in Equation (2) includes the effect of the geometrical distribution of the natural surfaces and the internal reflections. For plain surfaces, this term is negligible, but for heterogeneous and rough surfaces, such as forests, this term can reach a value of 2% (Sobrino *et al.* 1990). An approximation for $d_\varepsilon$ is

$$d_\varepsilon = (1 - \varepsilon_s)(1 - P_v) F \varepsilon_v \quad (4)$$

where, $F$ is a shape factor (Sobrino *et al.* 1990) whose mean value, assuming different geometrical distributions, is 0.55.

Vegetation products consist of the following:

(a) LAI, which was produced in this study by two methods to test their suitability for $ET_a$ estimation: using the equation proposed in SEBS help in ILWIS 3.8.3 Open, and with the equations proposed by Xavier & Vettorazzi (2004), respectively

$$LAI = \left[\frac{NDVI(1 + NDVI)}{1 - NDVI}\right]^{0.5} \quad (5)$$

$$LAI = a \times NDVI^b \quad (6)$$

where, $a$ and $b$ are regression parameters which varied for the months under investigation. Xavier & Vettorazzi (2004) reported $r^2$ of 0.54 to 0.74 for LAI estimation in their experiment.

(b) Percentage of vegetation ($P_v$), which was calculated by SEBS with Equation (3).

(c) Vegetation height ($h$), calculated in SEBS from the NDVI (Su 2002) when there is no field measurements

$$h = h_{min} + \frac{(h_{max} - h_{min})}{(NDVI_{veg} - NDVI_{soil})(NDVI - NDVI_{soil})} \quad (7)$$

where, $h_{min}$ and $h_{max}$ are the minimum and maximum vegetation heights in the region. SEBS suggests, respectively, 0.025 and 2.5 m. $NDVI_{veg}$ and $NDVI_{soil}$ are NDVI

of the fully vegetated and bare soil pixels, respectively. In this study, $h_{max}$ was set to 2.0 m corresponding to the plant height of *Atriplex* sp. stocks in pasture area. The maximum plant height in GBP refers to eucalyptus trees, which are higher than 5.0 m; however, this value as $h_{max}$ resulted in a non-realistic height map and was adjusted. In addition, $NDVI_{soil}$ was set as 0.05.

(d) Vegetation height ($h$) for the tree plantations was separately determined by field measurements and through a digitized map of $h$ generated for the area with trees. The polygonized map was then rasterized and added to the $h$ maps produced by the NDVI method for every image. SEBS was run with and without adding the forest height polygons on the generated height map (a merged map consisting of one made with Equation (7), and a digitized plant height in tree plantations) to check the effect of forest tree height on $ET_a$ calculation.

The zero plane displacement height ($d_0$) and the surface roughness height for momentum ($z_{om}$) are in general computed as a fraction of the plant height $h$. In SEBS, for ILWIS, the values for $d_0$ and $z_{om}$ can be either entered externally as an input map or as an attribute table associated with the land use map. If no map is entered, then $d_0$ and $z_{om}$ are calculated by the model. The tabulated values by Wierngа (1993) were used. As to the crucial impact of these parameters in obtaining an accurate reproduction of the surface fluxes (Su *et al.* 2005), considerable effort was made to prepare realistic maps of $d_0$ and $z_{om}$ based on the produced land use map for every image. A detailed classified land use map was prepared for every image on the basis of crop type and stage of growth based on available information and visual interpretation of that particular image acquisition date.

## Climatic data handling in SEBS

The temperature, humidity and wind data collected at the Gareh Bygone weather station were used. Air temperature and relative humidity for the time synchronized with the satellite overpass were calculated by interpolating the recorded data of 6:30 and 12:30. The mean daily temperature was calculated by averaging three standard times and absolute minimum and maximum data. Wind speed measurements were used as instantaneous and maximum daily wind parameters as described below. The Fasa weather station data were used for sunshine hours and air pressure. All of the parameters were entered as unique values in SEBS.

(1) Specific humidity $q$ (kg kg$^{-1}$), defined as the mass of water vapour per unit mass of moist air (Brutsaert 1982)

$$q = \frac{0.622 e_a}{[P - (1 - 0.622) e_a]} \tag{8}$$

where, 0.622 is the ratio of the molecular weights of water and dry air, $P$ is the total air pressure (hPa), and $e_a$ is the actual vapour pressure of the air (hPa) calculated as

$$e_a = e_s \frac{RH}{100} \tag{9}$$

where, RH is the relative humidity (%) and $e_s$ is the saturated vapour pressure (hPa). Estimation of $e_s$ can be (Monteith & Unsworth 2008):

$$e_s = \left[[10]^{-8.07-\left(1730\frac{63}{T+233.43}\right)}\right] \tag{10}$$

where, $T$ is temperature (°C). Values of $q$ in this study varied from 0.003 to 0.014 kg kg$^{-1}$.

(2) The wind speed parameter in SEBS, like the other RS based methods, is based on an instantaneous measurement at the time of the satellite overpass. As inferred by Mohammadnia & Kowsar (2003), the assumption of constant evaporative fraction can underestimate 24-h ET in arid climates where afternoon advection often increases with wind and may increase ET in proportion to $R_n$. In order to test the importance of maximum daily rather than instantaneous wind speed on daily $ET_a$, the following wind speed adjusted $u_{adj}$ function was adopted in this study

$$u_{adj} = u_{inst} + \left(\frac{u_{max}}{u_{inst}}\right) \tag{11}$$

where, $u_{inst}$ is instantaneous wind speed (m s$^{-1}$) at the time of satellite overpass, and $u_{max}$ is maximum daily wind speed (m s$^{-1}$). Incorporating maximum daily wind speed is due to the nature of wind occurrence in the study area. A tornado

type of wind normally occurs on summer days, mostly in the afternoon. Its effect on displacing the water vapour is not considered when the instantaneous wind speed is incorporated in the model. Average daily wind speed cannot truly reflect the impact of high wind speed occurrence. Thus Equation (11) adds a weighted value to the $u_{inst}$ which directly reflects high wind speed if it has occurred. Wind speed data measured at a height of 5 meters were converted to the 2 meter height using a logarithmic wind speed profile (Allen *et al.* 1998). Both sets of data ($u_{inst}$ and $u_{adj}$) were used as wind parameters separately to test the effect of maximum daily wind speed for improving $ET_a$ estimation.

Global solar radiation at the satellite overpass time can be inputted as spatially distributed (map), or as a measured value for a point which would be assigned to the whole area. SEBS has an internal module to estimate $R_n$ through the calculation of the incoming short wave and outgoing long wave radiation. Two types of input data were used in this study to test the sensitivity of the model to these data: (a) radiation measurements at Fasa weather station and (b) values generated by 'r.sun' inside GRASS (Table 3). The shadowing effect of the topography is optionally incorporated (http://grass.osgeo.org/grass64/manuals/r.sun.html).

$ET_a$ includes the effects of the climate through the reference evapotranspiration, $ET_o$, of the crop type through the crop coefficient ($K_c$), and of soil water stress through a stress coefficient ($K_s$) as described by Allen *et al.* (1998)

$$ET_a = K_s K_c ET_o \tag{12}$$

$K_c$ varies with the crop variety, crop growth stage, crop density and management and, only to a limited extent, with climate (Allen *et al.* 1998) for which an adjustment is used as a function of wind speed and minimum relative humidity. $K_c$, is influenced by surface residue and mulching (Martins *et al.* 2013). The estimated $ET_a$ of pixels located on the water reservoir inside the study area was selected for comparison against the calculated $ET_o$, considering that a $K_c$ of free water with a depth larger than 2 m approaches 1.05 (Allen *et al.* 1998). This approach was also used by Ahmad *et al.* (2006) in an arid region of India.

The daily $ET_o$ (mm day$^{-1}$) was calculated with variables observed at Gareh Bygone weather station with the FAO Penman–Monteith method (Allen *et al.* 1998)

$$ET_o = \frac{0,408\Delta(R_n - G) + \gamma \frac{900}{T+273} u_2 (e_s - e_a)}{\Delta + \gamma(1 + 0.34u_2)} \tag{13}$$

where, $R_n$ is net radiation at the reference crop surface (MJ m$^{-2}$ day$^{-1}$), $G$ is soil heat flux (MJ m$^{-2}$ day$^{-1}$), $T$ is mean daily air temperature at 2 m height (°C), $u_2$ is wind speed at 2 m height (m s$^{-1}$), $e_s$ is saturation vapour pressure (kPa), $e_a$ is actual vapour pressure (kPa), $\Delta$ is slope of vapour pressure curve (kPa°C$^{-1}$), $\gamma$ is psychrometric constant (kPa°C$^{-1}$). $e_s$ and $e_a$ were calculated as proposed by Allen *et al.* (1998), differently from Equations (9) and (10).

$ET_o$ was assumed as observed data owing to lack of measured $ET_a$. This approach is used in regions of scarce data, e.g., El Tahir *et al.* (2012) and Maeda *et al.* (2011).

**Table 3** | Comparing global radiation estimates from the 'r.sun' GRASS module and the Fasa weather station

| Statistics | Global radiation, Wm$^{-2}$ observed at Fasa weather station | Estimated with r.sun GRASS |
|---|---|---|
| Mean | 862.46 | 840.44 |
| Maximum | 1015.90 | 965.03 |
| Minimum | 615.10 | 561.36 |
| Standard deviation | 128.79 | 137.61 |
| No. samples | 18 | 18 |
| Standard error | | 53.75 |
| RSE | | 6.40% |
| Coefficient of determination | | 0.84 |
| Coefficient of regression | | 0.92 |

## Model parameterization and testing

To test the consistency of SEBS results and analysing the changes in SEBS parameters, different types of input maps and values were prepared and the model was run for every type of parameter while keeping all other parameters unchanged. The parameters and products used in this study are listed in Table 4. As there were numerous images and different types of input parameters and products, a script was written in order to facilitate the

**Table 4** | Sources of products and parameters for improving the SEBS

| Products and parameters | | Sources | |
|---|---|---|---|
| Basic RS products | Albedo | TOA | at-surface |
| | Emissivity | TOA | at-surface |
| | LST | TOA | at-surface |
| | NDVI | TOA | at-surface |
| Vegetation products | LAI | SEBS eq. | Eq. |
| | Height | SEBS eq. | SEBS eq. + TP polygons |
| | $f_c$ | SEBS eq. | |
| | $d_0$ and $z_{om}$ | Tabular | SEBS eq. |
| Climatic parameters | Wind speed | $U_{inst}$ | $U_{adj}$ |
| | Pressure | Instantaneous | |
| | Temp | Instantaneous | |
| | $q$ | Instantaneous | |
| *Global radiation* | | Weather station | r.sun GRASS |

LST is land surface temperature, TOA is top of atmosphere reflectance, at-surface is atmospherically corrected (at-surface) reflectance, LAI is leaf area index, SEBS eq. is the embedded equation in model, equation is LAI with Xavier & Vettorazzi (2004) equation, TP polygons is the measured tree heights and polygonizing TP area, $f_c$ is vegetation fraction, $d_0$ and $z_{om}$ are the displacement height and the roughness.

procedure. From the massive number of different possible parameter applications (9) and the number of analysed images (32), values of the pixels located on different land use pixels were extracted from the $ET_a$ maps. Statistical analyses of nine representative cases were selected for discussion. What is called 'case' here means a defined state of parameterization which is described in Table 4. The coefficient of determination ($r^2$) and the root mean square error (RMSE) were used to compare the modeled $ET_a$ against the calculated $ET_o$. The relative standard error (RSE), ratio of the standard error to the mean expressed as a percentage (Sokal & Rahlf 1995) was used to assess the r.sun computed against observed weather station global radiation.

## Deriving and adjusting $K_c$ values

The pixels' values of the radiation products relative to the Fasa weather station were extracted to compare them with the measured radiation. Since this station appeared only in the 162–40 satellite scenes, the number of compared pairs was only 18.

The best state of model parameterization, which led to the closer values to the calculated $ET_o$, was used for checking the $K_c$ of different land use types inside the region. The $K_c$ values were the ratios between $ET_a$ estimated by SEBS and $ET_o$. They were computed for several land uses including irrigated crops, eucalyptus plantations and pasture lands, and were compared with $K_c$ published in the literature. Wheat was selected as winter crop and forage corn as summer crop because of their dominance in the GBP. Other summer crops (Table 2) were ignored due to their reduced acreage. During the initial stage of crop growth $K_c$ mostly depends upon soil, water and wetting events. In the final stages, $K_c$ depends on crop management, e.g., purpose of harvesting. Thus, initial and end $K_c$ ($K_{c\ ini}$ and $K_{c\ end}$) cannot easily be compared with published $K_c$. The satellite overpass dates which coincided with the maximum canopy were selected to calculate mid-season $K_c$ ($K_{c\ mid}$). To take into account constraints in plant growth in irrigated crops (due to water stress, diseases and pests), the $K_{c\ mid}$ were adjusted using the LAI ratio (Allen *et al.* 1998) as follows:

$$K_{c\,adj} = K_{c\,mid(tabled)} - A_{cm} \tag{14}$$

with the empirical adjustment coefficient $A_{cm}$, given by

$$A_{cm} = 1 - (LAI_{stress}/LAI_{dense})^{0.5} \tag{15}$$

where, $K_{c\ adj}$ is the adjusted $K_{c\ mid}$, $LAI_{dense}$ is LAI for a crop having appropriate ground cover density, or maximum density, and $LAI_{stress}$ is the actual LAI of the crop when submitted to stress. Using this approach, $A_{cm} = 0$ when a crop is not stressed. In this study LAI in Equation (15) was replaced by NDVI because NDVI data were obtained from RS and the hypothesis of similarity between the concepts of NDVI and LAI could be accepted for the purpose of identification of crop stress. Following this procedure, the ratio between SEBS $ET_a$ and $ET_o$ is $K_{c\text{-}adj}$. Therefore, $K_c$ is calculated as

$$K_c = K_{c-adj} + A_{cm} \tag{16}$$

Values for $NDVI_{dense}$ were extracted from a well-managed irrigated farm belonging to the Agricultural Research Station of Darab (28°47′N, 54°19′E) located at 44 km northwest from the GBP, at the same altitude and with a similar climate and cropping season. Soil conditions and water quality are non-limiting at this farm, which produces the highest wheat yield of the region (above 6,000 kg ha$^{-1}$).

Crop coefficients for each crop type were finally compared with published $K_c$ to validate the RS model estimation similarly to procedures followed by Pôças *et al.* (2013). When the mid-season crop coefficients estimated by SEBS are close to the published $K_c$ it means that $ET_a$ estimation is adequate.

### Comparison with applied water

The volume of irrigation water was also measured in several fields in the area during the growth season. To do this, well discharge was measured in the head ditch above each field using a cut-throat flume (Walker 1989). This was then converted to seasonal volume of applied water per hectare using the time of application for each turn, the number of irrigations during the season, and the surface area irrigated.

Maps called 'cultivated farm field maps' were produced based on the farm field map for each image by employing NDVI. The NDVI value of cultivated farm fields (non-fallow) of every image date was found based on cultivation time table and expert knowledge. This value was used as a criterion for excluding the non-cultivated pixels of farm fields (i.e. fallow). The resulting maps were used for determining the size of cultivated area. The area of the maps for corresponding dates to each crop type was determined. Then the size of cultivation for each crop was multiplied by amount of applied water ($m^3$ per hectare) for that crop type to find out the total volume of applied water ($Mm^3$). The amount of efficient rainfall (recorded rainfall $\times$ 0.7) in volume base was then added to the calculated applied water.

To calculate the total amount of water used by ET, the $ET_a$ maps generated by SEBS were crossed with each cultivated farm field map, to calculate the weighted average of $ET_a$ for every image date. As the $ET_o$ was available as a daily base, the ratio $ET_o/ET_a$ for the image dates was used as a multiplier to calculate the $ET_a$ for the days between image intervals. Then, the daily $ET_a$ values were summed up for the cropping seasons.

## RESULTS AND DISCUSSION

### Radiation

Since Fasa weather station was located out of the 161–40 scene, the number of available observations of radiation was reduced to the images with non-cloudy conditions in the 162–40 scene, thus 21 scenes were available for radiation analysis and calculation.

An overview of the statistics for each of the graphs is presented in Table 3. The GRASS estimates of global radiation show a very good agreement with the measured radiation at Fasa, with a coefficient of determination $r^2$ of 0.84. RSE = 6.40% was obtained when net radiation is estimated with GRASS. Results for $r^2$ and RSE demonstrate the potential of GRASS r.sun module to estimate global radiation (Figure 4).

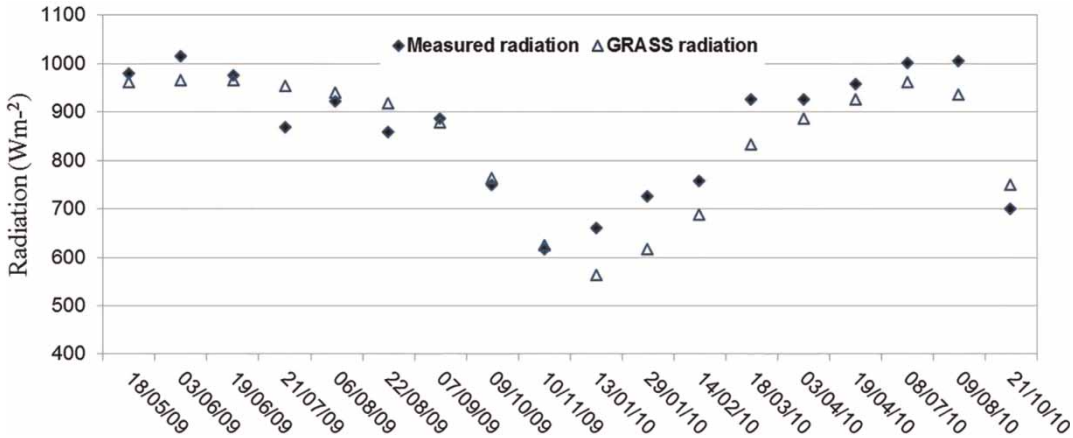


**Figure 4** | Comparing global radiation estimates by r.sun GRASS using Landsat data extracted for the pixel where the Fasa weather station is located with global radiation values measured at this station.

## Evapotranspiration

### Parameterization

Several alternatives for the analysis were tested. Each selected input (map product or parameter; Table 4) was changed and the model was run with all other inputs fixed. The goodness of fit when predicting $ET_a$ was not substantially changed in most cases. The cases when substantial changes occurred are presented in Table 5. Comparisons were made using data relative to pixels located on the water body, thus where the estimated $ET_a$ approximates $ET_o$. Table 6 shows that the mean values associated with different sources of $ET_a$ products are relatively stable. However, the variability of standard deviations is noticeable. The values of $r^2$ and RMSE illustrate the extent of agreement between the estimated $ET_a$ relative to water body pixels using different sources of parameterizations with the calculated FAO P-M $ET_o$. Improvements in prediction were obtained when replacing TOA with at-surface products, leading to an increase of 0.1 in $r^2$ and a decrease of 0.13 mm day$^{-1}$ in RMSE (column 4 in Table 5), thus inferring a positive impact of atmospheric correction in this study. By replacing radiation and LAI sources (columns 5 and 6 in Table 5), it can be assumed that the radiation map produced by GRASS and the LAI map generated with Equation (6) have more impact on the predictions than the other sources. Values of $r^2$ were then improved by 0.15 and RMSE by 0.18 mm day$^{-1}$. Results due to considering the maximum daily wind speed ($u_{adj}$) further produced an increase of 0.14 in $r^2$ and a decrease of 0.19 mm day$^{-1}$ in RMSE. Different sources of radiation and LAI led to a minor change. The best result was obtained with application of GRASS, at-surface product, with LAI derived by Equation (6) and using $u_{adj}$ resulting in an $r^2$ of 0.91. Results of the first step of prediction and the final improvement (respectively columns 3 and 7 in Table 5) are illustrated in Figure 5. The scattering of the points around the fitted line is improved when comparing before and after adjustment of the parameters. Ma *et al.* (2012) have also assessed SEBS-derived $ET_a$ against values measured with eddy covariance. Their study refers to a semi-arid region of South East Australia with annual rainfall averaging 384 mm and mean annual temperature of 19.9 °C, which is less dry than our study site. $r^2$ for their Landsat TM study was 0.95, which is close to our results of $r^2 = 0.91$.

To show the impact of incorporating the maximum daily wind speed (in terms of $u_{adj}$), the results of SEBS with $u_{inst}$

**Table 5** | Statistics of the evapotranspiration estimates from SEBS based on different sources of parameters or products

| Statistics | FAO P-M $ET_o$, (mm.day$^{-1}$) | SEBS ETa of water body pixels, mm.day$^{-1}$ | | | | |
|---|---|---|---|---|---|---|
| Mean | 6.5 | 5.65 | 6.12 | 6.52 | 6.31 | 6.74 |
| Std. deviation | 2.39 | 2.18 | 1.89 | 1.92 | 2 | 2.17 |
| Minimum | 2.24 | 1.72 | 2.1 | 2.47 | 2.34 | 2.73 |
| Maximum | 9.76 | 6.2 | 8.8 | 9.21 | 9.26 | 9.65 |
| No of samples | 32 | 32 | 32 | 32 | 32 | 32 |
| $R^2$ | | 0.53 | 0.62 | 0.68 | 0.77 | 0.91 |
| RMSE (mm.day$^{-1}$) | | 1.26 | 1.13 | 1.08 | 0.95 | 0.76 |
| Parameters* | | | | | | |
| Radiation | | Weather station | GRASS | GRASS | GRASS | GRASS |
| Basal RS product | | TOA | at-surf. | at-surf. | at-surf. | at-surf. |
| LAI | | SEBS eq. | SEBS eq. | SEBS eq. | Eq. | Eq. |
| Height | | SEBS + TP polygons | SEBS + TP polygons | SEBS | Eq. | Eq. |
| $d_0$ and $z_{om}$ | | SEBS | Tabular | Tabular | Tabular | Tabular |
| Wind speed | | $U_{inst.}$ | $U_{inst.}$ | $U_{inst.}$ | $U_{inst.}$ | $U_{adj}$ |

* Only the changes in products or parameters with substantial impact on improvement of the results are presented. TOA is top of atmosphere reflectance, at-surface is atmospherically corrected (at-surface) reflectance, SEBS eq. is the embedded equation in model, Eq. is LAI with Xavier & Vettorazzi (2004) equation, TP polygons is the measured tree heights and polygonizing TP area, $d_0$.

**Table 6** | Descriptive statistics of actual evapotranspiration computed from SEBS averaged for image dates and land use types

| Dates | FAO-PM $ET_o$ ($mm.day^{-1}$) | IC | TP | PI | PO | WB | BS |
|---|---|---|---|---|---|---|---|
| | | SEBS $ET_a$, mm.day-1 | | | | | |
| 11/05/09 | 7.90 | 5.19 | 4.91 | 3.49 | 2.65 | 8.10 | 1.30 |
| 18/05/09 | 7.22 | 4.47 | 4.07 | 2.66 | 2.04 | 7.87 | 1.03 |
| 27/05/09 | 7.67 | 5.00 | 4.83 | 3.49 | 2.75 | 8.84 | 1.38 |
| 03/06/09 | 7.57 | 3.45 | 2.91 | 1.75 | 0.95 | 8.31 | 0.46 |
| 19/06/09 | 8.44 | 4.96 | 4.72 | 3.41 | 2.96 | 8.29 | 1.46 |
| 28/06/09 | 8.62 | 4.91 | 4.08 | 2.95 | 2.37 | 9.26 | 1.10 |
| 14/07/09 | 9.76 | 5.93 | 6.24 | 4.58 | 4.08 | 8.63 | 2.07 |
| 21/07/09 | 9.56 | 5.70 | 6.50 | 4.87 | 4.21 | 9.06 | 2.16 |
| 30/07/09 | 8.59 | 5.61 | 6.70 | 4.99 | 4.47 | 8.57 | 2.22 |
| 06/08/09 | 9.32 | 4.78 | 6.01 | 4.34 | 3.82 | 9.15 | 1.97 |
| 15/08/09 | 9.50 | 6.21 | 7.43 | 5.63 | 5.13 | 8.58 | 2.60 |
| 22/08/09 | 9.67 | 2.48 | 2.65 | 1.93 | 1.32 | 9.65 | 0.72 |
| 31/08/09 | 8.00 | 4.72 | 6.00 | 4.26 | 3.63 | 7.91 | 1.89 |
| 07/09/09 | 8.06 | 3.48 | 3.54 | 2.79 | 2.21 | 7.53 | 1.18 |
| 16/09/09 | 6.85 | 3.36 | 3.79 | 2.54 | 1.93 | 6.92 | 1.01 |
| 02/10/09 | 5.03 | 3.33 | 4.01 | 2.61 | 2.21 | 6.37 | 1.20 |
| 09/10/09 | 5.69 | 2.90 | 3.15 | 2.15 | 1.60 | 5.45 | 0.85 |
| 18/10/09 | 4.82 | 3.14 | 3.80 | 2.61 | 2.19 | 5.37 | 1.15 |
| 03/11/09 | 3.89 | 1.26 | 1.18 | 0.72 | 0.41 | 3.29 | 0.25 |
| 10/11/09 | 3.23 | 2.51 | 2.83 | 1.82 | 1.43 | 3.69 | 0.74 |
| 13/01/10 | 2.24 | 2.41 | 2.83 | 2.32 | 2.05 | 3.01 | 1.00 |
| 22/01/10 | 2.36 | 1.21 | 1.92 | 1.68 | 1.38 | 3.07 | 0.65 |
| 29/01/10 | 2.48 | 3.32 | 3.78 | 3.14 | 2.72 | 4.03 | 1.32 |
| 14/02/10 | 2.46 | 2.46 | 2.34 | 1.67 | 1.54 | 2.73 | 0.72 |
| 23/02/10 | 3.89 | 3.32 | 2.23 | 1.23 | 1.52 | 4.21 | 0.81 |
| 18/03/10 | 5.58 | 5.32 | 2.93 | 1.58 | 0.57 | 6.12 | 0.26 |
| 03/04/10 | 5.84 | 6.06 | 3.28 | 1.86 | 1.20 | 6.78 | 0.74 |
| 19/04/10 | 5.22 | 6.51 | 6.05 | 4.98 | 4.82 | 7.15 | 2.37 |
| 28/04/10 | 8.07 | 4.82 | 1.70 | 0.69 | 0.41 | 7.67 | 0.27 |
| 08/07/10 | 8.55 | 5.70 | 6.34 | 4.75 | 4.35 | 9.40 | 2.21 |
| 12/10/10 | 6.07 | 2.69 | 2.45 | 1.43 | 1.02 | 5.85 | 0.54 |
| 21/10/10 | 5.85 | 2.10 | 1.91 | 0.97 | 0.55 | 4.98 | 0.31 |
| Average | 6.50 | 4.04 | 3.97 | 2.81 | 2.33 | 6.75 | 1.19 |

Statistics are the average data of all representative points of each land use (illustrated in Figure 2). FAO P-M $ET_0$ is FAO Penman–Monteith reference crop ET; IC is irrigated crops; TP is tree plantations; PI is pastures inside the FWS; PO is pastures outside the FWS; WB is water body; BS is bare soil.

and $u_{adj}$ are presented in Figure 6. The maximum differences between graphs of SEBS $ET_a$ (extracted from water body pixels) and FAO P-M $ET_o$ occurred in July and August, mainly in 2009 (Figure 5). After incorporating maximum daily wind speed, the differences became substantially smaller for these months (which is also inferred from $r^2$ and RMSE changes from column 3 to 7 in Table 5). The largest deviation between SEBS's $ET_a$ and FAO P-M $ET_o$ was observed on 6 July 2009 (7.29 vs. 9.32 mm $day^{-1}$, respectively). The maximum wind speed on this day was 12.3 m $s^{-1}$ as compared with the instantaneous satellite overpass time wind speed of 3.5 m $s^{-1}$. After considering the maximum wind speed, the corresponding results become much closer (9.15 vs. 9.32 mm $day^{-1}$). These results are likely due to the possible occurrence of advection in the area, as reported by Raziei & Pereira (2013).

## Spatial and temporal variability of $ET_a$

Descriptive data of temporal and spatial changes in $ET_a$ for various land uses are presented in Table 6. It shows that temporal changes in predicted $ET_a$ from all main land uses logically follow the seasons. A minimum $ET_a$ in January is followed by an increasing trend until maximum values occur in June–October, which is followed by a decreasing trend until the next year's minimum, in January. Variations of $ET_a$ for various land use types are also shown in Table 6. $ET_a$ of tree plantations remains higher than for the other land use types on all dates except those corresponding to high demand periods of irrigated crops, e.g., by 18/03/2010 and 03/04/2010. The $ET_a$ values from pastures located inside the FWS (PI) are generally higher than $ET_a$ of pastures from outside (PO).

The rasterized map of vegetation height when overlayed on that of the NDVI-derived height for each date originates a map of the vegetation height. However, running SEBS with this map resulted in non-realistic values of $ET_a$ for the tree plantations' area. Changing the other input parameters did not improve these $ET_a$ estimations for the tree plantations' pixels. Consequently, the resulting $ET_a$ calculations for the area are based on the NDVI-derived height map considered in SEBS and where the maximum height is adjusted.

Edraki *et al.* (2007) observed $ET_a$ for the same tree plantations' site in GBP (*Eucalyptus camaldulensis* Dehnh) in three plots, each having nine 6-year-old trees. These authors performed a soil water balance for 180 cm depth using a

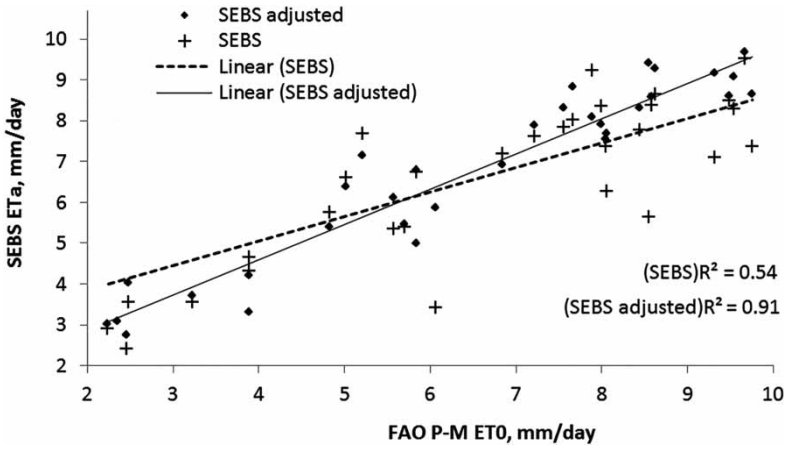


**Figure 5** | Relating $ET_a$ computed with SEBS for water body pixels with $ET_o$ computed with the FAO P-M equation when: (SEBS) using radiation observed at Fasa weather station, TOA reflectance, internal LAI and $d_0$ and $Z_{om}$ of SEBS and instantaneous wind speed, and (SEBS adjusted), using r.sun GRASS-radiation, at-surface reflectance, LAI with Xavier & Vettorazzi (2004) equation, $d_0$ and $z_{om}$ of attribute table and adjusted wind speed.

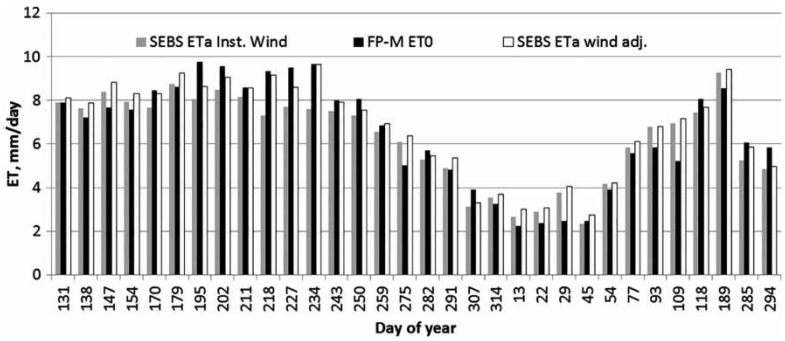


**Figure 6** | Comparing daily $Et_a$ computed with SEBS for water body pixels (based on at-surface reflectance products) with FAO P-M $ET_o$ when using: instantaneous wind speed ($u_{inst}$), and adjusted wind speed ($u_{adj}$) incorporating maximum daily wind speed.

neutron probe in the period 31 March to 27 August 1991. The reported daily ET ranged from 0.2 to 6.1 mm $d^{-1}$ and 0.1 to 7.5 mm $d^{-1}$ for two of the plots; results for the third one show large errors. The SEBS calculated daily $ET_a$ values for the tree plantations ranged between 1.2 and 7.4 mm $d^{-1}$ (Table 6), and are thus in agreement with referred results by Edraki *et al.* (2007). Roberts & Rosier (1993) reported transpiration rates of 1.0 to 5.5 mm $d^{-1}$ for 2-year-old *E. camaldulensis* trees in Bangalore, India. Cramer *et al.* (1999) reported transpiration measured with the sap flow method in Queensland, Australia, in 4- to 6-year-old *E. camaldulensis*; reported results ranged from 1.0 to 4.5 mm $d^{-1}$ depending on the season and density of plantations. Since results refer to transpiration only, they are close to observations in the current study.

## Crop coefficients

While $ET_a$ varies enormously in time and space and is not comparable among different locations, average crop coefficients are normalized and may be transferable from one site to another. Thus, they are comparable when averaged (Allen *et al.* 1998). In this study, daily $K_c$ values are obtained but comparisons are only valid when referring to averaged values. However, there is the need to understand when extreme values may be justified by local or regional advection or if they result from SEBS overestimation of $ET_a$. That possible overestimation is noted by various authors, e.g., Lu *et al.* (2013).

Results of daily $K_c$ calculations for winter wheat and forage corn are presented in Table 7. The calculated $K_c$ in

**Table 7** | Daily estimates of mid-season crop coefficients obtained from SEBS-derived $ET_a$ and $ET_o$

| Crops | Dates | FAO P-M $ET_o$, mm.day$^{-1}$ | SEBS* $ET_a$, mm.day$^{-1}$ | $K_{c\text{-adj}}$ | NDVI* | $NDVI_{dens}$ | $A_{cm}$ | $K_c$ |
|---|---|---|---|---|---|---|---|---|
| Wheat | 23/02/10 | 3.89 | 4.21 | 1.08 | 0.74 | 0.82 | 0.05 | 1.13 |
| | 18/03/10 | 5.58 | 5.91 | 1.06 | 0.70 | 0.88 | 0.11 | 1.17 |
| | 03/04/10 | 5.84 | 6.78 | 1.16 | 0.83 | 0.86 | 0.02 | 1.18 |
| | 19/04/10 | 5.22 | 6.88 | 1.32 | 0.75 | 0.79 | 0.03 | 1.34 |
| | Average | 5.13 | 5.95 | 1.16 | 0.76 | 0.84 | 0.05 | 1.21 |
| Forage corn | 07/09/09 | 8.06 | 6.63 | 0.82 | 0.66 | 0.78 | 0.08 | 0.91 |
| | 16/09/09 | 6.85 | 5.89 | 0.86 | 0.67 | 0.82 | 0.10 | 0.96 |
| | 02/10/09 | 5.03 | 6.30 | 1.25 | 0.72 | 0.85 | 0.08 | 1.33 |
| | 09/10/09 | 5.69 | 5.29 | 0.93 | 0.67 | 0.81 | 0.09 | 1.02 |
| | 18/10/09 | 4.82 | 5.37 | 1.11 | 0.62 | 0.74 | 0.08 | 1.19 |
| | Average | 6.09 | 5.90 | 1.00 | 0.67 | 0.80 | 0.09 | 1.08 |

* Averaged data from 10 fields with proper management.

the last column is obtained from RS data with Equation (16). Daily values for winter wheat $K_{c\ mid}$ were in the range of 1.13–1.34, averaging 1.21. The maximum daily $K_{c\ mid}$ value was 1.34, which is above the expected averaged $K_{c\ mid}$ for wheat but is likely to occur on a day when atmospheric demand is high, mainly if advection occurs. Zaitchik *et al.* (2007) reported positive advective heating rates in plateaus around the Zagros mountains, where GBP is located. Advection was also reported by Malek (1987) relative to the Fars Province, the region where the study area is located, particularly from April to September. GBP has hot, dry and windy days during the mid-season of wheat (Table 1). It is surrounded by large areas of sparse and dry natural vegetation where the sensible heat flux, H, largely dominates over the latent heat flux, $\lambda$E, thus contributing to produce heat of the air transported by the wind into the cultivated areas. Assuming the advection definition of McIlroy & Angus (1964), and considering the information reported by Malek (1987) & Zaitchik *et al.* (2007), advection is likely to occur in the area. Because $ET_o$ is computed considering only vertical energy fluxes, advection is considered in $K_c$ values (Allen *et al.* 1998). Hence, the averaged $K_{c\ mid}$ value of 1.21 compares well with typical values reported in the literature; a range of 1.08–1.19 is reported in several studies referring to a variety of climates (Bandyopadhyay & Mallick 2003; Li *et al.* 2003; Kjaersgaard *et al.* 2008; Gao *et al.* 2009; Ko *et al.* 2009; López-Urrea *et al.* 2009; Zhao *et al.* 2013). Niazi *et al.* (2005) reported $K_{c\ mid}$ values of 1.09–1.13 at Zarghan, also in Fars Province, but with a less dry climate and located at a higher altitude (1,621 m.a.s.l.), which justifies the small $K_c$ difference (in addition to crop varieties and crop techniques adopted).

The $K_{c\ mid}$ for forage corn averaged 1.08 while daily estimated values varied between 0.91 and 1.33 (Table 7). Similarly to what occurred with the wheat $K_{c\ mid}$, the high daily value of 1.33 is likely to be due to advection, which may be stronger during the maize crop season than that occurring during the wheat season. Several authors reported similar but generally larger values than the estimated $K_{c\ mid} = 1.08$ for grain maize, e.g., Allen *et al.* (1998) proposed a value of 1.20, Gao *et al.* (2009), Martínez-Cob (2008) and Piccinni *et al.* (2009) reported 1.19–1.20, while Zhao *et al.* (2013) obtained a value of 1.15. Values similar to those in this study are reported by Rosa *et al.* (2012) and Liu & Pereira (2000), respectively 1.10 and 1.08. Gheysary *et al.* (2006) reported $K_{c\ mid}$ of 1.13 for a study developed at Varamin, South Tehran. It is therefore likely that the values obtained are appropriate; differences may also be due to the crop variety and management practices used.

The time series of $K_c$ for tree plantations presented in Figure 7(a) refers to four locations having different density of vegetation, from very dense to sparse. As mentioned in the study area description, *Eucalyptus camaldulensis* is the predominant species in the FWS project covering more than 90% of the forested area. Furthermore, as Kowsar (1991) explained in detail, the majority of the trees

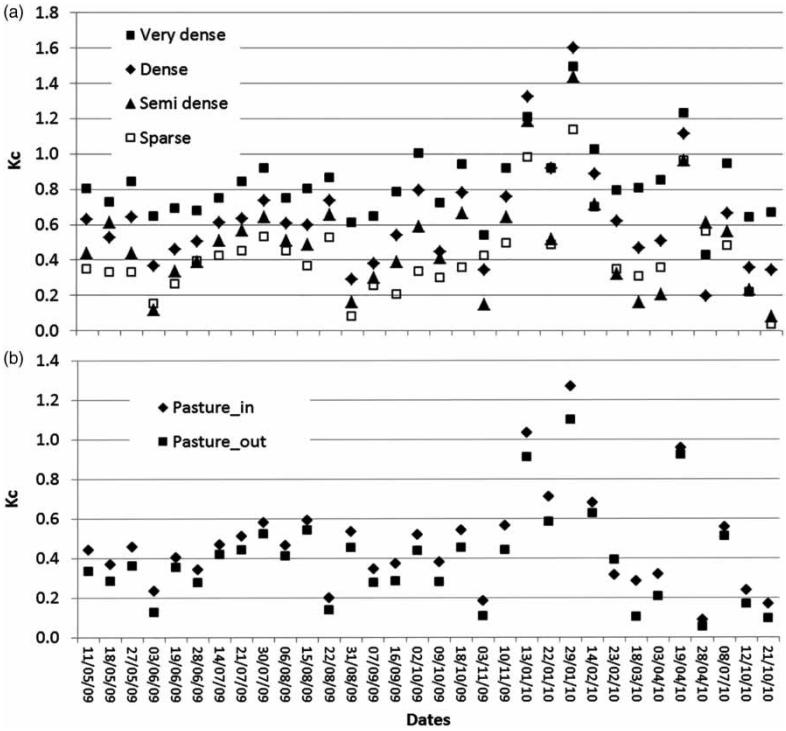


**Figure 7** | Time series of $K_c$ values calculated for tree plantations (a) and pasture area (b).

were planted in 1983–1984. The main important difference is regarding plantation density and we consider this for our analysis. Table 7 shows the change in $K_c$ as influenced by density. As expected, the $K_c$ values decrease with reduced plant density (0.83–0.42). Very dense vegetation pixels have shown the highest $K_c$ values. The very dense vegetation pixels refer to an area where water is available for most of the year because of flooding. Pôças *et al.* (2013) reported $K_c = 0.68$ for evergreen forests, mainly consisting of *Pinus pinaster*; Attarod *et al.* (2011) described a $K_c$ of 0.93 for a Japanese red pine forest; Hou *et al.* (2010) reported $K_c =$ 0.62 for *Populus euphratica*; and Allen *et al.* (1998) proposed $K_{c\ mid}$ of 1.0 for conifer trees. Thus, $K_c$ values below 1.0 are in agreement with the literature. However, daily $K_c$ peaks occurred by January, February and April, which are quite high but acceptable if resulting from advection as discussed above with reference to Malek (1987) and Zaitchik *et al.* (2007).

Temporal changes in $K_c$ values for pasture lands are presented in Figure 7(b). Peaks are shown for the same dates as for eucalyptus trees, which supports the hypothesis of advection during those days. Peaks also occur for the periods previous to cuts. Mean $K_c$ values are 0.47 and 0.39 for PI and PO, respectively. For irrigated pastures, the $K_c$ values found by Pôças *et al.* (2013) using RS data were 0.88–0.89, thus much higher than those obtained in this study. Various studies reported by these authors also show $K_c$ higher than most of the values shown in Table 7. However, values for non-irrigated pastures are smaller, for instance, Aase *et al.* (1973) described $K_c$ of 0.55 for native vegetation with sparse cover ground in Montana. A $K_c$ of 0.45 is reported for steppe grasslands of Mongolia (Yang & Zhou 2011). The $K_c$ for the pasture outside the FWS seems to be overestimated. Some recent investigations have also proposed overestimation of $ET_a$ by SEBS in the conditions of water deficit in soil surface as the source of ET (Gibson *et al.* 2011; Lu *et al.* 2013).

All of the generated ET maps show a reasonable distribution of ET throughout the study site, differing in ET extent according to the seasons. As an example, two representative final ET maps of winter and summer conditions are presented in Figure 8.

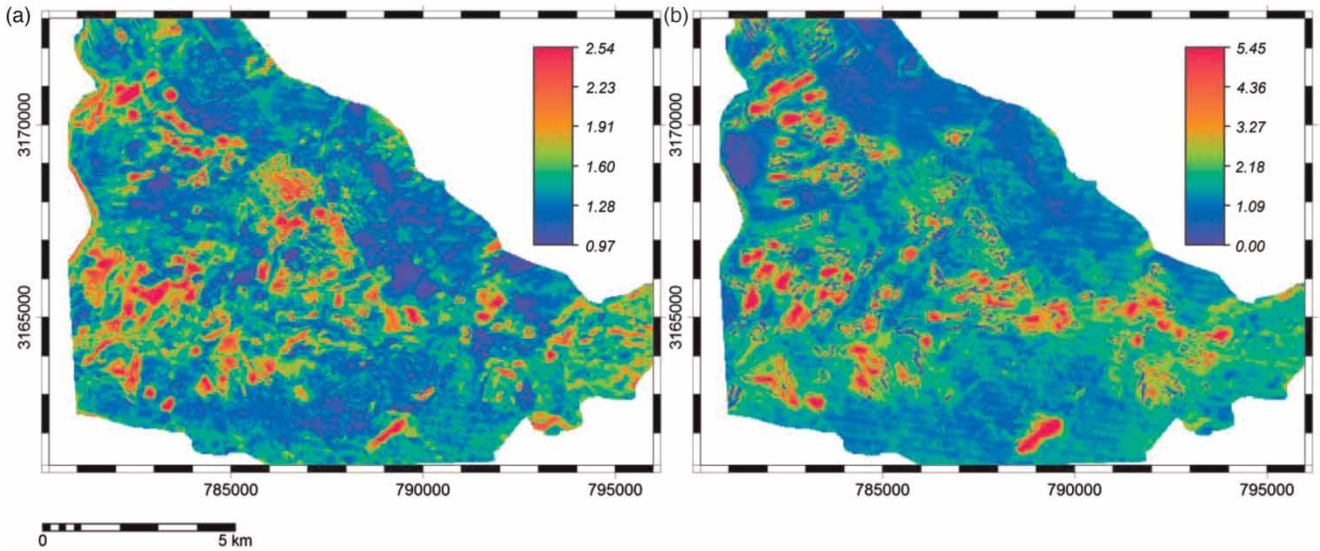


**Figure 8** | Actual ET maps of the Gareh Bygone Plain generated with SEBS for (a) low farming season 10/11/2009 and (b) high farming season 03/04/2010.

## Water consumption comparison

The amount of water consumption calculated by the method is presented in Table 8. In the water year 2009–2010, from the 2,200 ha of farm fields in GBP, an average of 1,234 ha was used for winter crops and 716 ha for summer crops with the remainder remaining uncultivated. The amount of applied water to the cultivated farms is calculated as 15.94 $Mm^3$ and the summation of yearly consumption by ET, excluding the recorded rainfall, is 10.98 $Mm^3$. The difference (4.97 $Mm^3$ or 31% of applied water) may be considered as irrigation returned flow which is percolated from the root zone. In other words, the efficiency of irrigation is determined as 69.9% which is reasonable for this irrigation system in GBP. This is also in the range of the reported values for the main crops in dry regions of New Mexico, USA – 16–56% (average 25%) for returned flow (Sabol *et al.* 1987).

**Table 8** | Water consumption calculations

| | | | Effective rainfall[1] | | |
|---|---|---|---|---|---|
| **Crops** | **Area (ha)** | **Average applied ($m^3.ha^{-1}$)** | **mm** | **($m^3$.ha-1)** | **Consumed water ($Mm^3$)** |
| Based on measured applied water | | | | | |
| Winter crops | 1,234 | 4,800 | 172.9 | 1729.0 | 8.06 |
| Summer crops | 716 | 11,000 | – | – | 7.88 |
| Sum | | | | | 15.94 |
| | **Area (ha)** | **Yearly ET ($m^3.ha^{-1}$)** | | | **Consumed water ($Mm^3$)** |
| Based on SEBS $ET_a$[2] | | | | | |
| Winter crops | 1,234 | 3,900 | | | 4.81 |
| Summer crops | 716 | 8,600 | | | 6.16 |
| Sum | | | | | 10.97 |

[1]Amount of recorded rainfall × 0.7.
[2]Amount of recorded rainfall (volume base) is subtracted from the total $ET_a$ calculations.

## CONCLUSIONS

The use of the SEBS model for the arid landscape of southern Iran was performed with improved parameterization for estimates relative to net radiation and wind speed. Due to high winds in the area an adjustment was done to consider the maximum daily wind speed. After improved parameterization, SEBS $ET_a$ relative to water pixels compared well with reference $ET_o$.

The validation of SEBS-derived $ET_a$ was performed through analysing the crop coefficients obtained as ratios of $ET_a$ to the reference $ET_o$ relative to main crop vegetation in the area. While $ET_a$ varies in time and space and is not comparable among different locations, crop coefficients are normalized and may be transferable from one site to another. Thus, time averaged $K_c$ are comparable. Daily $K_c$ values were computed and therefore only their averaged values for the mid-season could be compared with those reported in the literature. An overestimation in $K_c$ value for sparse vegetation (out of FWS) pasture area is inferred from this study. Moreover, extreme $K_c$ values could be considered non-erroneous since they could be due to local and regional advection. Water consumption by cultivated crops based on SEBS results compared well with that calculated by measured applied water and as a consequence a reasonable calculated irrigation returned flow. Thus, the SEBS estimation of $ET_a$ and consequent $K_c$ is useful for performing an adequate assessment of the FWS project as well as to be used further in water management in the region. SEBS can now be applied as a tool for monitoring the impact of various land use scenarios in GBP, including those aimed at adaptation to climate change. However, it is advisable that ground observations be further developed to better assess SEBS and control uncertainties in its parameterization.

## ACKNOWLEDGEMENTS

Part of the study is supported by SUMAMAD project financed by Flemish Government of Belgium and UNESCO which are cordially acknowledged. The former International Centre of Water for Food Security (under auspices of Charles Sturt University, Australia), and Fars Research Center for Agriculture and Natural Resources in Iran are appreciated for providing the working environment and necessary facilities to conduct this research. Thanks are also due to Dr Yan Chemin who bestowed valuable guidance in both the theory and application of ET mapping based on RS.

## REFERENCES

Aase, J. K., Wight, J. R. & Siddoway, F. H. 1973 Estimating soil water content on native rangeland. *Agric. Meteorol.* **12**, 185–191.

Ahmad, M., Biggs, T., Turral, H. & Scott, C. 2006 Application of SEBAL approach and MODIS time-series to map vegetation water use patterns in the data scarce Krishna river basin of India. *Water Sci. Technol.* **53**, 83–90.

Allen, R. G., Pereira, L. S., Raes, D. & Smith, M. 1998 FAO Irrigation and Drainage Paper No. 56, Crop evapotranspiration (guidelines for computing crop water requirements). Food and Agriculture Organization of the United Nations, Rome, Italy.

Allen, R. G., Pereira, L. S., Howell, T. A. & Jensen, M. E. 2011 Evapotranspiration information reporting: I. Factors governing measurement accuracy. *Agric. Water Manag.* **98** (6), 899–920.

Allen, R. G., Tasumi, M. & Trezza, R. 2007 Satellite-based energy balance for mapping evapotranspiration with internalized calibration (METRIC)-model. *J. Irrig. Drain. E-ASCE* **133**, 380–394.

Attarod, P., Aoki, M., Bayramzadeh, V. & Ahmadi, M. T. 2011 Micrometeorological observations above a Japanese red pine forest within the growing season. *Turk. J. Agric. For.* **35**, 597–609.

Bandyopadhyay, P. K. & Mallick, S. 2003 Actual evapotranspiration and crop coefficients of wheat (Triticum aestivum) under varying moisture levels of humid tropical canal command area. *Agric. Water Manage.* **59**, 33–47.

Bastiaanssen, W. G. M., Menenti, M., Feddes, R. A. & Holtslag, A. A. M. 1998 A remote sensing surface energy balance algorithm for land (SEBAL). 1. Formulation. *J. Hydrol.* **212–213**, 198–212.

Brutsaert, W. 1982 *Evaporation into the Atmosphere*. D. Reidel Publishing Company, Dordrecht, The Netherlands.

Carlson, T. N. & Ripley, D. A. 1997 On the relation between NDVI, fractional vegetation cover, and leaf area index. *Remote Sens. Environ.* **62**, 241–252.

Chander, G. & Markham, B. 2003 Revised Landsat-5 TM radiometric calibration procedures and postcalibration dynamic ranges. *IEEE Trans. Geosci. Remote* **41**, 2674–2677.

Chehbouni, A., Nouvellon, Y., Lhomme, J. P., Watts, C., Boulet, G., Kerr, Y. H., Moran, M. S. & Goodrich, D. C. 2001 Estimation of surface sensible heat flux using dual angle observations of radiative surface temperature. *Agric. Forest Meteorol.* **108**, 55–65.

Courault, D., Seguin, B. & Olioso, A. 2005 Review on estimation of evapotranspiration from remote sensing data: From

empirical to numerical modeling approaches. *Irrig. Drain. Syst.* **19**, 223–249.

Cramer, V. A., Thorburn, P. J. & Fraser, G. W. 1999 Transpiration and groundwater uptake from farm forest plots of Casuarina glauca and Eucalyptus camaldulensis in saline areas of southeast Queensland, Australia. *Agric. Water Manage.* **39**, 187–204.

Edraki, M., Kowsar, S., Mehrbakhsh, A. & Bordbar, A. 2007 Water consumption of a six-year-old river red gum plantation in the Southern Zagros Mountains, Iran. *J. Mountain Sci.* **4**, 136–145.

El Tahir, M., Wenzhong, W., Xu, C., Youjing, Z. & Singh, V. 2012 Comparison of methods for estimation of regional actual evapotranspiration in data scarce regions: Blue Nile region, Eastern Sudan. *J. Hydrol. Eng.* **17**, 578–589.

Gao, Y., Duan, A., Sun, J., Li, F., Liu, Z., Liu, H. & Liu, Z. 2009 Crop coefficient and water-use efficiency of winter wheat/spring maize strip intercropping. *Field Crops Res.* **111**, 65–73.

Gheysary, M., Mirlatifi, M., Homaee, M. & Asadi, M. E. 2006 Determination of crop water use and crop coefficient of corn silage based on crop growth stages (in Farsi with English abstract). *J. Agric. Eng. Res.* **7**, 125–142.

Gibson, L. A., Münch, Z. & Engelbrecht, J. 2011 Particular uncertainties encountered in using a pre-packaged SEBS model to derive evapotranspiration in a heterogeneous study area in South Africa. *Hydrol. Earth Syst. Sci.* **15**, 295–310.

Gowda, P. H., Chavez, J. L., Colaizzi, P. D., Evett, S. R., Howell, T. A. & Tolk, J. A. 2008 ET mapping for agricultural water management: present status and challenges. *Irrigation Sci.* **26**, 223–237.

Hashemi, H., Berndtsson, R. & Kompani-Zare, M. 2012 Steady-state unconfined aquifer simulation of the Gareh-Bygone Plain, Iran. *Open Hydrol. J.* **6**, 58–67.

Hou, L. G., Xiao, H. L., Si, J. H., Xiao, S. C., Zhou, M. X. & Yang, Y. G. 2010 Evapotranspiration and crop coefficient of Populus euphratica Oliv forest during the growing season in the extreme arid region northwest China. *Agric. Water Manage.* **97**, 351–356.

Kalma, J. D., McVicar, T. R. & McCabe, M. F. 2008 Estimating land surface evaporation: a review of methods using remotely sensed surface temperature data. *Surv. Geophys.* **29**, 421–469.

Kjaersgaard, J. H., Plauborg, F., Mollerup, M., Petersen, C. T. & Hansen, S. 2008 Crop coefficients for winter wheat in a sub-humid climate regime. *Agric. Water Manage.* **95**, 918–924.

Ko, J., Piccinni, G., Marek, T. & Howell, T. 2009 Determination of growth-stage-specific crop coefficients (Kc) of cotton and wheat. *Agric. Water Manage.* **96**, 1691–1697.

Kowsar, S. A. 1991 Floodwater spreading for desertification control: an integrated approach. *Desrtification Control Bulletin* **19**, 3–18.

Kowsar, A. & Pakparvar, M. 2003 Assessment methodology for establishing an Aquitopia, Islamic Republic of Iran. In: *Proceedings of the Second International Workshop on Sustainable Management of Marginal Drylands (SUMAMAD) (pp. 40–55.)*. UNU, UNESCO, Shiraz, Iran.

Li, Y.-L., Cui, J.-Y., Zhang, T.-H. & Zhao, H.-L. 2003 Measurement of evapotranspiration of irrigated spring wheat and maize in a semi-arid region of north China. *Agric. Water Manage.* **61**, 1–12.

Liu, Y. & Pereira, L. 2000 Validation of FAO methods for estimating crop coefficients. *Trans. CSAE* **16**, 26–30.

López-Urrea, R., Montoro, A., González-Piqueras, J., López-Fuster, P. & Fereres, E. 2009 Water use of spring wheat to raise water productivity. *Agric. Water Manage.* **96**, 1305–1310.

Lu, J., Li, Z.-L., Tang, R., Tang, B.-H., Wu, H., Yang, F., Labed, J. & Zhou, G. 2013 Evaluating the SEBS-estimated evaporative fraction from MODIS data for a complex underlying surface. *Hydrol. Process.* **27**, 3139–3149.

Ma, W., Hafeez, M., Rabbani, U., Ishikawa, H. & Ma, Y. 2012 Retrieved actual ET using SEBS model from Landsat-5 TM data for irrigation area of Australia. *Atmospheric Environment* **59**, 408–414. doi:http://dx.doi.org/10.1016/j.atmosenv.2012.05.040.

Maeda, E. E., Wiberg, D. A. & Pellikka, P. K. 2011 Estimating reference evapotranspiration using remote sensing and empirical models in a region with limited ground data availability in Kenya. *Appl. Geogr.* **31**, 251–258.

Malek, E. 1987 Comparison of alternative methods for estimating ETp and evaluation of advection in the Bajgah area, Iran. *Agric. Forest Meteorol.* **39**, 185–192.

Martínez-Cob, A. 2008 Use of thermal units to estimate corn crop coefficients under semiarid climatic conditions. *Irrigation Sci.* **26**, 335–345.

Martins, J. D., Rodrigues, G. C., Paredes, P., Carlesso, R., Oliveira, Z. B., Knies, A. E., Petry, M. T. & Pereira, L. S. 2013 Dual crop coefficients for maize in southern Brazil: Model testing for sprinkler and drip irrigation and mulched soil. *Biosyst. Eng.* **115**, 291–310.

McCabe, M. F. & Wood, E. F. 2006 Scale influences on the remote estimation of evapotranspiration using multiple satellite sensors. *Remote Sens. Environ.* **105**, 271–285.

McIlroy, I. C. & Angus, D. E. 1964 Grass, water and soil evaporation at Aspendale. *Agric. Meteorol.* **1**, 201–224.

Menenti, M. 1984 Physical aspects and determination of evaporation in deserts applying remote sensing techniques. Report 10, Institute of Land and Water Management Research, (IWC), Wageningen, The Netherlands. *Zeitschrift für Pflanzenernährung und Bodenkunde* **149**, 142–143.

Menenti, M. & Choudhury, B. J. (eds) 1993 *Parameterization of land surface evapotranspiration using a location dependent potential evapotranspiration and surface temperature range: IAHS Publ 212*. IAHS Press, Wallingford, UK.

Mesbah, S. H. & Kowsar, S. A. 2010 Spate irrigation of rangelands: a drought mitigation mechanism. In: *Encyclopedia of Agricultural Production* (F. C. Wager, ed.). Nova Science Publishers, Hauppauge, NY, pp. 489–528.

Mohammadnia, M. & Kowsar, S. A. 2003 Clay translocation in the artificial recharge of a groundwater system in the southern Zagros Mountains, Iran. *Mt. Res. Dev.* **23**, 50–55.

Monteith, J. & Unsworth, M. 2008 *Principles of Environmental Physics*. Academic Press, Burlington, VT.

Neteler, M. & Mitasova, H. 2008 *Open Source GIS: A GRASS GIS Approach*. Springer, New York.

Niazi, J., Fooladmand, H. R., Ahmadi, S. H. & Vaziri, J. 2005 Water requirement and crop coefficient of wheat in Zarghan Area, Fars Province (in Farsi with English abstract). *J. Sci. Technol. Agric. Nat. Resour., Water Soil Sci.* **9**, 1–7.

Norman, J. M., Kustas, W. P. & Humes, K. S. 1995 Source approach for estimating soil and vegetation energy fluxes in observations of directional radiometric surface temperature. *Agric. Forest Meteorol.* **77**, 263–293.

OFCM 2005 Federal Meteorological Handbook No. 1 – Surface Weather Observations and Reports. Office of the Federal Coordinator of Meteorology, Washington DC.

Overgaard, J., Rosbjerg, D. & Butts, M. 2006 Land-surface modelling in hydrological perspective – a review. *Biogeosciences* **3**, 229–241.

Piccinni, G., Ko, J., Marek, T. & Howell, T. 2009 Determination of growth-stage-specific crop coefficients (KC) of maize and sorghum. *Agric. Water Manage.* **96**, 1698–1704.

Pôças, I., Cunha, M., Pereira, L. S. & Allen, R. G. 2013 Using remote sensing energy balance and evapotranspiration to characterize montane landscape vegetation with focus on grass and pasture lands. *Int. J. Appl. Earth Obs. Geoinf.* **21**, 159–172.

Raziei, T. & Pereira, L. S. 2013 Estimation of $ET_0$ with Hargreaves–Samani and FAO-PM temperature methods for a wide range of climates in Iran. *Agric. Water Manag.* **121**, 1–18. doi:http://dx.doi.org/10.1016/j.agwat.2012.12.019.

Roberts, J. & Rosier, P. T. W. 1993 Physiological studies in young Eucalyptus stands in southern India and derived estimates of forest transpiration. *Agric. Water Manage.* **24**, 103–118.

Roerink, G. J., Su, Z. & Menenti, M. 2000 S-SEBI: A simple remote sensing algorithm to estimate the surface energy balance. *Phys. Chem. Earth B* **25**, 147–157.

Rosa, R. D., Paredes, P., Rodrigues, G. C., Alves, I., Fernando, R. M., Pereira, L. S. & Allen, R. G. 2012 Implementing the dual crop coefficient approach in interactive software. 1. Background and computational strategy. *Agric. Water Manag.* **103**, 8–24.

Sabol, G., Bouwer, H. & Wierenga, P. 1987 Irrigation effects in Arizona and New Mexico. *J. Irrig. Drain. Eng.* **113**, 30–48.

Sobrino, J., Caselles, V. & Becker, F. 1990 Significance of the remotely sensed thermal infrared measurements obtained over a citrus orchard. *J. Photogr. Remote Sens.* **44**, 343–354.

Sobrino, J. A., Jiménez-Muñoz, J. C. & Paolini, L. 2004 Land surface temperature retrieval from LANDSAT TM 5. *Remote Sens. Environ.* **90**, 434–440.

Sokal, R. R. & Rahlf, J. F. 1995 *Biometry: The Principles and Practice of Statistics in Biological Research*. W. H. Freeman & Co, San Francisco, CA.

Su, Z. 2002 The Surface Energy Balance System (SEBS) for estimation of turbulent heat fluxes. *Hydrol. Earth Syst. Sci.* **6**, 85–99.

Su, H., McCabe, M. F., Wood, E. F., Su, Z. & Prueger, J. H. 2005 Modeling evapotranspiration during SMACEX: Comparing two approaches for local- and regional-scale prediction. *J. Hydrometeorol.* **6**, 910–922.

Su, Z., Timmermans, W., Gieske, A., Jia, L., Elbers, J. A., Olioso, A., Timmermans, J., Van Der Velde, R., Jin, X., Van Der Kwast, H., Nerry, F., Sabol, D., Sobrino, J. A., Moreno, J. & Bianchi, R. 2008 Quantification of land–atmosphere exchanges of water, energy and carbon dioxide in space and time over the heterogeneous Barrax site. *Int. J. Remote Sens.* **29** (17–18), 5215–5235.

Sun, Z., Wang, Q., Matsushita, B., Fukushima, T., Ouyang, Z. & Watanabe, M. 2009 Development of a Simple Remote Sensing EvapoTranspiration model (Sim-ReSET): Algorithm and model test. *J. Hydrol.* **376**, 476–485.

Tasumi, M., Allen, R. G. & Trezza, R. 2008 At-surface reflectance and albedo from satellite for operational calculation of land surface energy balance. *J. Hydrol. Eng.* **13**, 51–63.

van der Kwast, J., Timmermans, W., Gieske, A., Su, Z., Olioso, A., Jia, L., Elbers, J., Karssenberg, D. & de Jong, S. 2009 Evaluation of the Surface Energy Balance System (SEBS) applied to ASTER imagery with flux-measurements at the SPARC 2004 site (Barrax, Spain). *Hydrol. Earth Syst. Sci.* **13** (7), 1337–1347. doi:http://dx.doi.org/10.5194/hess-13-1337-2009.

Walker, W. R. (ed.) 1989 *Guidelines for designing and evaluating surface irrigation systems*. FAO, Rome, Italy.

Wiernga, J. 1993 Representative roughness parameters for homogeneous terrain. *Boundary-Layer Meteorol.* **63**, 323–363.

Xavier, A. & Vettorazzi, C. 2004 Mapping leaf area index through spectral vegetation indices in a subtropical watershed. *Int. J. Remote Sens.* **25**, 1661–1672.

Yang, F. & Zhou, G. 2011 Characteristics and modeling of evapotranspiration over a temperate desert steppe in Inner Mongolia. *J. Hydrol.* **396**, 139–147.

Zaitchik, B. F., Evans, J. P. & Smith, R. B. 2007 Regional impact of an elevated heat source: the Zagros Plateau of Iran. *J. Climate* **20**, 4133–4146.

Zhao, N., Liu, Y., Cai, J., Paredes, P., Rosa, R. D. & Pereira, L. S. 2013 Dual crop coefficient modelling applied to the winter wheat–summer maize crop sequence in North China Plain: Basal crop coefficients and soil evaporation component. *Agric. Water Manage.* **117**, 93–105.

First received 13 December 2013; accepted in revised form 12 May 2014. Available online 12 June 2014